LETTERS

Phosphate oxygen isotopic evidence for a temperate and biologically active Archaean ocean

Ruth E. Blake[1], Sae Jung Chang[1] & Aivo Lepland[2,3]

Oxygen and silicon isotope compositions of cherts[1–3] and studies of protein evolution[4] have been interpreted to reflect ocean temperatures of 55–85 °C during the early Palaeoarchaean era (~3.5 billion years ago). A recent study combining oxygen and hydrogen isotope compositions of cherts, however, makes a case for Archaean ocean temperatures being no greater than 40 °C (ref. 5). Ocean temperature can also be assessed using the oxygen isotope composition of phosphate. Recent studies show that ^{18}O:^{16}O ratios of dissolved inorganic phosphate ($\delta^{18}O_P$) reflect ambient seawater temperature as well as biological processing that dominates marine phosphorus cycling at low temperature[6,7]. All forms of life require and concentrate phosphorus, and as a result of biological processing, modern marine phosphates have $\delta^{18}O_P$ values typically between 19–26‰ (VSMOW)[7,8], highly evolved from presumed source values of ~6–8‰ that are characteristic of apatite in igneous rocks[9,10] and meteorites[11]. Here we report oxygen isotope compositions of phosphates in sediments from the 3.2–3.5-billion-year-old Barberton Greenstone Belt in South Africa. We find that $\delta^{18}O_P$ values range from 9.3‰ to 19.9‰ and include the highest values reported for Archaean rocks. The temperatures calculated from our highest $\delta^{18}O_P$ values and assuming equilibrium with sea water with $\delta^{18}O = 0$‰ (ref. 12) range from 26 °C to 35 °C. The higher $\delta^{18}O_P$ values are similar to those of modern marine phosphate and suggest a well-developed phosphorus cycle and evolved biologic activity on the Archaean Earth.

Geochemical fingerprints of early life[13–15] and ancient ocean chemistry may be found in the relatively well-preserved rocks of the Barberton Greenstone Belt—3.2–3.5 billion years old—in southern Africa[16] (Supplementary Figs 1 and 2). The Barberton Greenstone Belt comprises a sequence of volcanic rocks, inter-layered with volumetrically minor sedimentary units consisting of cherts, banded iron formations and variably silicified terrigenous and volcaniclastic sediments[16], which have experienced only low-grade metamorphism[17]. The cherts have been variably interpreted to be of hydrothermal origin, sedimentary precipitates, the products of early diagenetic replacement of pyroclastic sediments, or derived from the interaction of seafloor sediments with silica-saturated Archaean sea water[1,18–20].

A longstanding controversy exists over the interpretation of the oxygen-isotope compositions of Precambrian cherts and the co-existing phosphates that systematically decrease with increasing age[1,2]. Low $\delta^{18}O$ values of Barberton cherts have been attributed to (1) diagenetic /hydrothermal alteration by low-$\delta^{18}O$ fluids[19,20], (2) equilibrium with $\delta^{18}O = 0$‰ sea water and very high (55–85 °C) ocean temperatures[1] or (3) equilibrium with $\delta^{18}O = -10$‰ sea water and low (<40 °C) ocean temperatures[5]. Modelled variations in $\delta^{30}Si$ values of cherts were initially interpreted to support high-temperature (~70 °C) oceans 3.5 billion years ago on the basis of the temperature dependence of silica solubility[3]. A more recent study[21] however, challenges this interpretation and suggests that $\delta^{30}Si$ values do not record high-temperature early Archaean oceans, but rather the influence of hydrothermal fluids.

The new $\delta^{18}O$ analyses of Barberton phosphates and derived temperatures presented here come from outcrop samples of sedimentary units (cherts, banded iron formations, silicified tuffs and silicified sandstone) at various stratigraphic levels (Supplementary Information). Thin-section analyses revealed the presence of discrete phosphate phases only in some samples, consistent with generally low P_2O_5 content ranging from <0.01 to 0.04 wt% (Supplementary

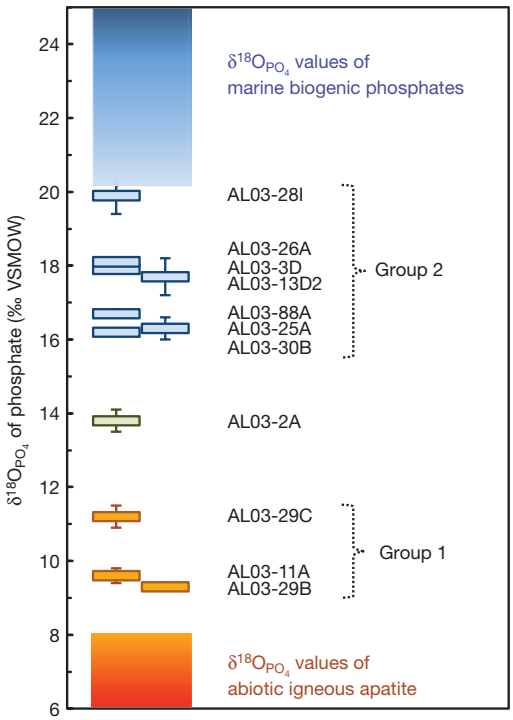

Figure 1 | Comparison of $\delta^{18}O_P$ values from Barberton sediments with modern marine phosphates[7,8] and igneous phosphates[9,10]. Isotopically heavy Group 2 samples have modern-day marine phosphate $\delta^{18}O_P$ values of 17.7–19.9‰ and record biological processing and equilibrium with cool ocean surface waters. Group 1 samples have been affected by secondary veining (Fig. 2a) and their low $\delta^{18}O_P$ values of 9.3–11.2‰ record high-temperature phosphate. Data points between Groups 1 and 2 and in the lower range of Group 2 may reflect mixtures of secondary hydrothermal–metamorphic apatite and primary sedimentary phosphate not fully resolved by our petrographic and sequential extraction methods. Error bars represent standard deviation based on replicate mass spectrometric analyses of single samples (Supplementary Table 1).

[1]Yale University, Department of Geology and Geophysics, New Haven, Connecticut 06520-8109, USA. [2]Geological Survey of Norway, 7491 Trondheim, Norway. [3]Tallinn Technical University, Institute of Geology, 19086 Tallinn, Estonia.

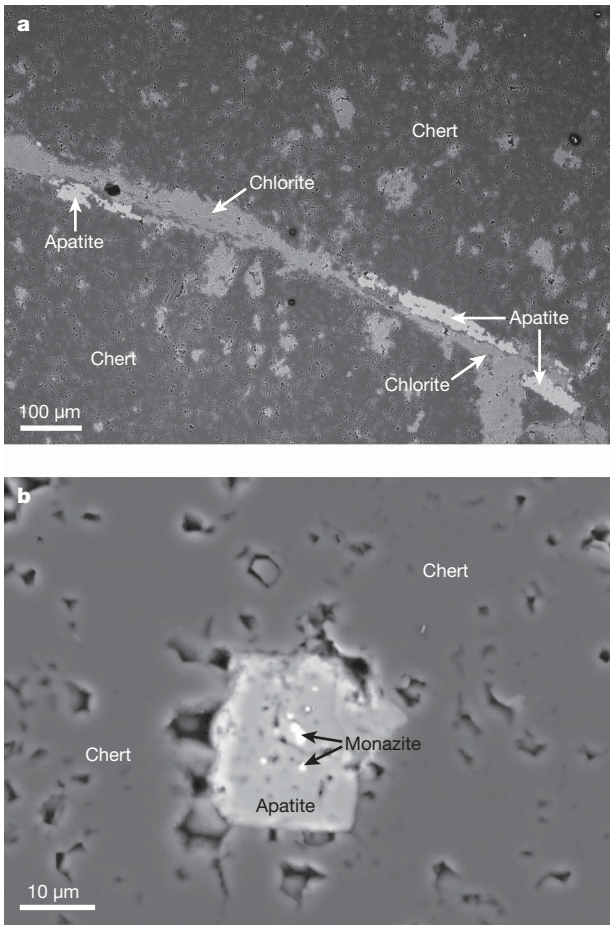

Figure 2 | Back-scattered electron images of phosphate phases in Barberton sediments. **a**, Apatite in cross-cutting chlorite vein in AL03-29B. Samples affected by such secondary veining contain isotopically light phosphate formed during hydrothermal or metamorphic alteration. **b**, Apatite crystal with monazite inclusion in AL03-28C. Disseminated, apatite crystals not related to veins have been identified in some samples, particularly ferruginous cherts and banded iron formations. Phosphate is isotopically heavy in such samples, reflecting a sedimentary origin and cool ambient sea water.

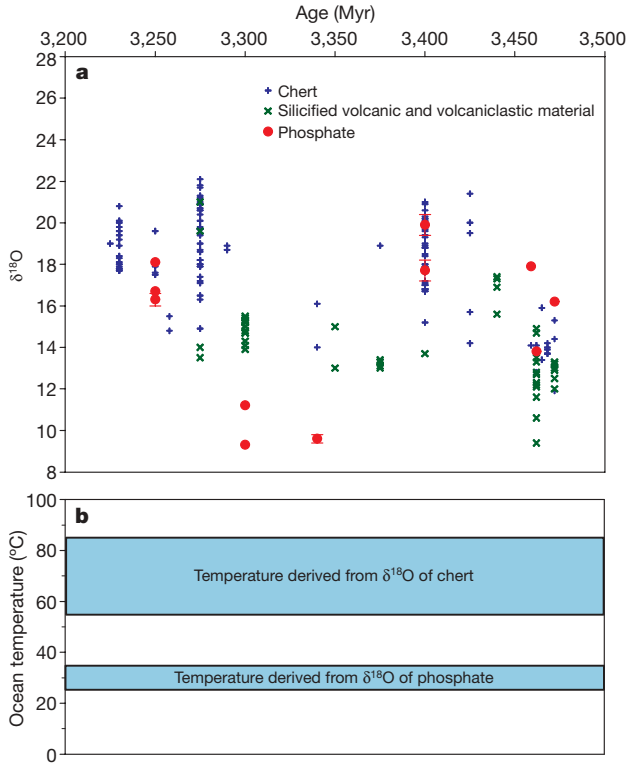

Figure 3 | Comparison of $\delta^{18}O$ values of Barberton phosphates and cherts. Comparison of $\delta^{18}O$ values of Barberton phosphates (this study) and cherts and silicified volcanic and volcaniclastic materials[1] (**a**) with estimates of ocean temperature derived from $\delta^{18}O$ values of chert and phosphate (**b**). If phosphate and chert co-precipitated in equilibrium with the same sea water, phosphate should be >8‰ lighter than co-existing chert ($\Delta^{18}O_{chert\text{-}phosphate}$ >8‰) at seawater temperatures below 70 °C (refs 1, 2, 26). But the $\Delta^{18}O_{chert\text{-}phosphate}$ is considerably smaller, indicating isotopic disequilibrium between phosphate and cherts. This disequilibrium can be explained by decoupled formation in a thermally stratified ocean: phosphate $\delta^{18}O$ records biological processing and equilibrium with cooler surface waters, while chert $\delta^{18}O$ records hydrothermal influence and warmer conditions at the sea floor (Fig. 4). The error bars represent standard deviation based on replicate mass spectrometric analyses of single samples (Supplementary Table 1).

Table 1). Phosphate was extracted from powdered whole-rock samples, purified and converted to silver phosphate for oxygen-isotope analysis using the method of ref. 22 (see Methods). All oxygen-isotope data are reported relative to the Vienna Standard Mean Ocean Water (VSMOW) in per mil (‰).

Previous studies reporting $\delta^{18}O$ analyses of trace amounts of phosphate do not specify the mode of occurrence of PO_4 (such as apatite or other mineral phosphates or organophosphorus). We tested Barberton samples explicitly for the presence of condensed or organic phosphates using ^{18}O-labelled water to prepare extractant solutions. We also used a sequential extraction method and microanalysis technique that provided insight into the occurrence and specific associations (such as apatite veins and PO_4 associated with iron), of the small amounts of PO_4 present in most samples (Methods and Supplementary Table 1).

The $\delta^{18}O_P$ values of Barberton sediments range from 9.3‰ to 19.9‰ (Fig. 1 and Supplementary Table 1) and can be divided into two groups: 9.3–11.2‰ (Group 1) and 16.2–19.9‰ (Group 2), with one value of 13.8‰ that falls between the two defined groups. Phosphate in Group 1 samples could be extracted almost entirely using 10 M nitric acid (HNO_3), whereas the fraction of PO_4 extracted with 6 M hydrochloric acid (HCl) was only 2.4–10.6% of the total PO_4. This result suggests that phosphate in Group 1 samples is present as apatite, which is consistent with petrographic observations that identify the presence of relatively large apatite crystals in cross-cutting veinlets within Group 1 samples (Fig. 2a).

Group 2 samples are typically rich in iron (Fe_2O_3 from 8–50 wt%) with the exception of AL03-3D and AL03-30B. Phosphate has a well-known strong affinity for iron oxides in marine and aquatic systems[23]. Iron oxides have been shown to record $\delta^{18}O_P$ values of dissolved inorganic phosphate in ambient sea water[7] with no measurable fractionation between dissolved inorganic phosphate and iron-oxide-bound PO_4 (Supplementary Table 2). Consistent with a high iron-oxide content, HCl was more effective than HNO_3 for the extraction of PO_4 from Group 2 samples, presumably owing to the formation of Fe–Cl^{n+}(aq) complexes that increase iron solubility. The amount of PO_4 extracted from iron-rich Group 2 samples by 6 M HCl was greater than 63% of the total PO_4 with the exception of sample AL03-30B. This result suggests that phosphate in Group 2 samples is predominantly associated with iron oxides (for example, adsorbed, occluded and/or co-precipitated), although phosphorus and Fe abundances are not linearly correlated in all samples. Minor phosphate in some Group 2 samples occurs as disseminated apatite crystals that occasionally contain inclusions of monazite (Fig. 2b). Trace amounts of monazite and xenotime that are present in some samples would be insoluble in both HNO_3 and HCl solutions.

$\delta^{18}O_P$ values of 9.3–11.2‰ for Group 1 phosphates are close to, but slightly higher than, the range reported for igneous and metamorphic apatites[9,10] (Fig. 1). These relatively low $\delta^{18}O_P$ values,

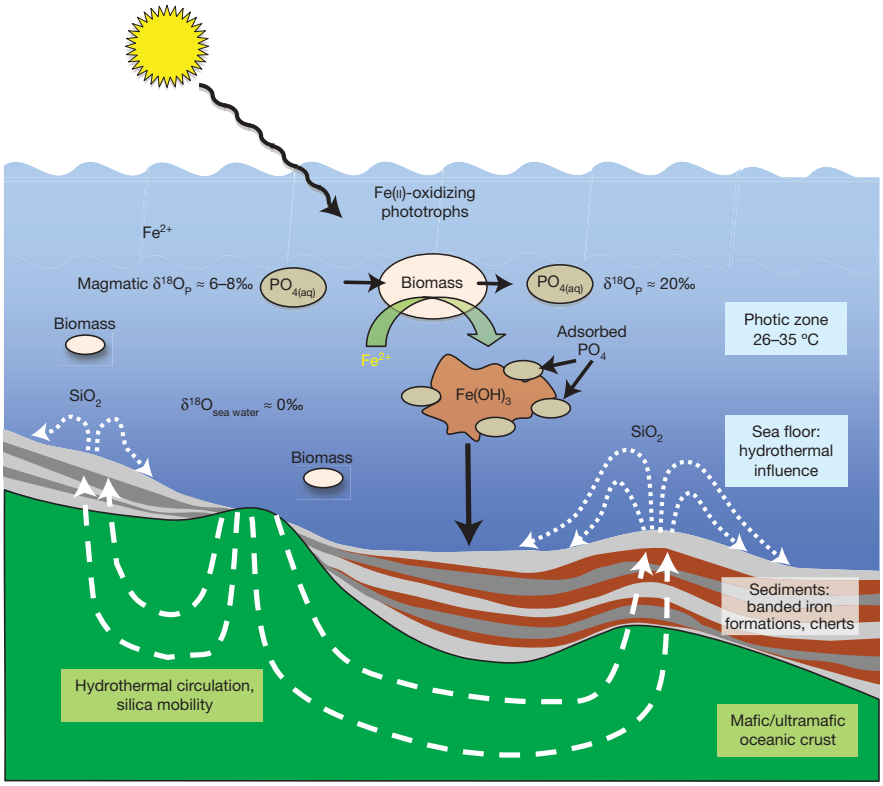

Figure 4 | Sketch of possible phosphorus cycling and phosphate–iron oxide interactions in a thermally stratified Archaean ocean. Biologically processed dissolved phosphate, perhaps involving Fe^{2+} oxidizing anoxygenic phototrophs, records equilibrium $\delta^{18}O_P$ values with cooler ocean surface waters. Dissolved phosphate is scavenged by iron oxides and is carried along with sinking biomass from the photic zone to the shallow and deep sea floor, where some cherts are formed under higher-temperature conditions.

together with evidence for secondary veining and phosphate mobility (Fig. 2a), indicate that Group 1 phosphates are mainly formed from hydrothermal or metamorphic fluids. The $\delta^{18}O_P$ value of 9.3‰ for sample AL03-29B was the lowest of all the samples analysed in this study and thus may represent an end-member value for PO_4 derived from secondary fluids.

$\delta^{18}O_P$ values of 16.2‰ to 19.9‰ for phosphate in Group 2 are close to those of modern marine phosphate[7,8] (Fig. 1). Karhu and Epstein[2] reported a similarly high $\delta^{18}O_P$ value of 17.9‰ for one Barberton chert sample, but this measurement was dismissed as anomalous. Several high $\delta^{18}O_P$ values among Group 2 samples, however, demonstrate that such phosphates are not anomalous but instead probably common, and may be typical for primary sedimentary phosphate in Barberton sediments. The range in $\delta^{18}O_P$ of Group 2 samples can be explained by minor interactions with secondary fluids that variably shifted $\delta^{18}O_P$ to slightly lower values.

Ocean temperatures calculated from O isotope proxies using chert or phosphate depend on the value used for $\delta^{18}O$ of water ($\delta^{18}O_W$). It has been suggested that in the absence of glacial periods, $\delta^{18}O_W$ of sea water has remained constant near a value of about 0‰ over geologic time[12] (see more detailed discussion in Supplementary Information). Oxygen isotope and trace element compositions and alteration patterns in volcanic rocks from the Barberton Greenstone Belt have also been interpreted to reflect ~0‰ Archaean seawater $\delta^{18}O$ values[20,24]. In contrast, it has been proposed that the $\delta^{18}O_W$ of sea water has evolved to present-day values relatively systematically over time from values as low as −10‰ to −13‰ in the Archaean[5,25].

If Group 2 phosphates with the highest $\delta^{18}O_P$ values (17.7 to 19.9‰) formed in isotopic equilibrium with 0‰ sea water, the calculated[26] Archaean ocean temperature ranges from 26 °C to 35 °C. A calculation using the proposed $\delta^{18}O_W$ values of −10‰ to −13‰ and $\delta^{18}O_P$ values of 17.7–19.9‰ gives unrealistic ocean temperatures (−8 to −30°C), so such low $\delta^{18}O_W$ values of Archaean sea water are not compatible with the $\delta^{18}O_P$ record. $\delta^{18}O_W$ values as low as −8.0‰ are compatible with our highest $\delta^{18}O_P$ values at very cold ocean temperatures (1 °C). A more temperate 30 °C ocean would yield a minimum $\delta^{18}O_W$ value of −1.2‰, as constrained by $\delta^{18}O_P$.

If both chert and phosphate precipitated in equilibrium with the same sea water and retained their primary isotopic compositions, the $\delta^{18}O$ values of cherts should be >8‰ higher than co-existing phosphates at temperatures <70 °C (refs 1, 2, 26). Thus, chert formed in equilibrium with 0‰ sea water and phosphates having $\delta^{18}O_P$ values of 17.7–19.9‰ would, at <70 °C, have $\delta^{18}O$ values higher than 26–28‰. No $\delta^{18}O$ values higher than 22.1‰ have been reported for Barberton cherts[1,5], and in some units, phosphates are isotopically heavier than co-occurring cherts[2] (Fig. 3a).

The disequilibrium between Barberton phosphates and cherts can be explained either by extensive secondary overprinting that has led to non-equilibrium resetting of primary $\delta^{18}O$ values, or by decoupling of initial formation of phosphates and cherts. The ability of phosphates to retain primary $\delta^{18}O_P$ values through burial diagenesis and over geologic timescales is evident in the recording of palaeotemperatures and seasonal fluctuations in $\delta^{18}O_P$ by fossil apatites[8,27]. Exchange of sedimentary phosphates with heavy diagenetic/metamorphic fluids or fluids that evolved in the presence of isotopically heavy cherts could potentially result in ^{18}O enrichment of reworked phosphates. This, however, would cause phosphate $\delta^{18}O$ values to shift towards, but not exceed, co-occurring chert values, and thus would not account for the isotopic compositions of some sedimentary units for which phosphate $\delta^{18}O$ values are higher than those of coexisting cherts[2] (Fig. 3a).

At low to moderate temperatures, only biological processes have been shown to cause large shifts in $\delta^{18}O_P$ values of dissolved inorganic PO_4 (refs 6 and 7) and apatite[8] that can account for the evolution of $\delta^{18}O_P$ from igneous PO_4 source values by as much as 15–20‰, to reach modern-marine values in the range 18–26‰. Hence we propose that high $\delta^{18}O_P$ values of 17.7–19.9‰ in Barberton phosphates are the

result of the exchange of oxygen between dissolved PO_4 and sea water ($\delta^{18}O_W = 0‰$) at low temperatures (26–35 °C), driven by enzymatic catalysis and microbial metabolism of phosphorus in the Archaean ocean.

Since the discovery of anoxygenic phototrophs capable of using Fe^{2+} as an electron donor[28], it has been suggested that such organisms could have been responsible for the widespread accumulation of banded iron formations before the oxygenation of Earth's oceans and atmosphere[29]. In the vicinity of Fe oxyhydroxides, produced either as a by-product of anoxygenic photosynthesis, or by alternative abiotic mechanisms involving dissolved O_2 or ultraviolet photolysis in surface waters, any dissolved phosphate would be rapidly adsorbed[30]. The oxygen-isotope ratio of PO_4 scavenged by Fe-oxyhydroxide particles as well as that of degrading biomass carried from the photic zone to the sea floor would reflect the biological cycling and temperature regime of surface waters[7]. Thus, the observed isotopic disequilibrium between phosphates and co-existing cherts can be explained by decoupled formation of these phases, with cherts being possibly affected by hydrothermal processes at the sea floor[19–21] regardless of water depth. Accordingly, high phosphate $\delta^{18}O$ would record low-temperature biological processing and equilibrium with cooler surface waters, while some chert $\delta^{18}O$ values could record warmer seafloor conditions (Fig. 4). Such thermal stratification would be best developed in deeper-water settings, which, in the Barberton Greenstone Belt, are characterized by accumulation of ferruginous cherts and banded iron formations, consistent with typically high $\delta^{18}O_P$ values in ferruginous sediments. Near modern-day $\delta^{18}O$ values of 17.7–19.9‰ for dissolved marine phosphate in Barberton sediments thus provide new evidence that the Archaean ocean was cool and that the marine phosphate reservoir and biological cycling of phosphorus had already evolved significantly by 3.5 billion years ago.

METHODS SUMMARY

This study was made possible by newly developed techniques with which to measure $\delta^{18}O_P$ that reduce sample requirements from ~50 μmol to only 5 μmol PO_4 and allow quantitative precipitation of small amounts of silver phosphate from a large and complex rock matrix. Phosphate was sequentially extracted from whole-rock samples using HNO_3 and HCl, purified by recrystallization and ion resin exchange, then converted to silver phosphate for oxygen isotope analysis. Isotope analyses were carried out at the Earth System Center for Stable Isotope Studies (ESCSIS) at Yale using a Thermo-Chemolysis Elemental Analyser (TC/EA, 1,350 °C) coupled to a Delta +XL continuous-flow isotope ratio monitoring mass spectrometer (Thermo-Finnigan) with precision of ±0.2–0.3‰. Phosphate oxygen-isotope ratios were calibrated against conventional fluorination using three silver phosphate standards according to published methods[22]. The $\delta^{18}O_P$ value of a KH_2PO_4 internal laboratory standard ($14.4 \pm 0.5‰$, s.d., $n = 5$) treated with the same phosphate extraction, purification and precipitation methods as the samples is at the accepted value ($14.2 \pm 0.3‰$, s.d., $n = 5$) (Supplementary Table 1), demonstrating that the sample purification process does not introduce artefacts.

Full Methods and any associated references are available in the online version of the paper at www.nature.com/nature.

Received 10 May 2009; accepted 18 February 2010.

1. Knauth, L. P. & Lowe, D. R. High Archean climatic temperature inferred from oxygen isotope geochemistry of cherts in the 3.5 Ga Swaziland Supergroup, South Africa. *Geol. Soc. Am. Bull.* **115,** 566–580 (2003).
2. Karhu, J. & Epstein, S. The implication of the oxygen isotope records in coexisting cherts and phosphates. *Geochim. Cosmochim. Acta* **50,** 1745–1756 (1986).
3. Robert, F. & Chaussidon, M. A palaeotemperature curve for the Precambrian oceans based on silicon isotopes in cherts. *Nature* **443,** 969–972 (2006).
4. Gaucher, E. A., Govindarajan, S. & Ganesh, O. K. Paleotemperature trend for Precambrian life inferred from resurrected proteins. *Nature* **451,** 704–707 (2008).
5. Hren, M. T., Tice, M. M. & Chamberlain, C. P. Oxygen and hydrogen isotope evidence for a temperate climate 3.42 billion years ago. *Nature* **462,** 205–208 (2009).
6. Blake, R. E., O'Neil, J. R. & Surkov, A. V. Biogeochemical cycling of phosphorus: insights from oxygen isotope effects of phosphoenzymes. *Am. J. Sci.* **305,** 596–620 (2005).
7. Colman, A. S., Blake, R. E., Karl, D. M., Fogel, M. L. & Turekian, K. K. Marine phosphate oxygen isotopes and organic matter remineralization in the oceans. *Proc. Natl Acad. Sci. USA* **102,** 13023–13028 (2005).
8. Shemesh, A., Kolodny, Y. & Luz, B. Oxygen isotope variations in phosphate of biogenic apatites. II. Phosphorite rocks. *Earth Planet. Sci. Lett.* **64,** 405–416 (1983).
9. Taylor, H. P. & Epstein, S. Relationship between O^{18}/O^{16} ratios in coexisting minerals of igneous and metamorphic rocks. Part I. Principles and experimental results. *Geol. Soc. Am. Bull.* **73,** 461–480 (1962).
10. Markel, D., Kolodny, Y., Luz, B. & Nishri, A. Phosphorus cycling and phosphorus sources in Lake Kinneret: tracing by oxygen isotopes in phosphate. *Isr. J. Earth Sci.* **43,** 165–178 (1994).
11. Greenwood, J. P., Blake, R. E. & Coath, C. D. Ion microprobe measurements of $^{18}O/^{16}O$ ratios of phosphate minerals in the Martian meteorites ALH84001 and Los Angeles. *Geochim. Cosmochim. Acta* **67,** 2289–2298 (2003).
12. Muehlenbachs, K. & Clayton, R. N. Oxygen isotope composition of the oceanic crust and its bearing on seawater. *J. Geophys. Res.* **81,** 4365–4369 (1976).
13. Walsh, M. M. & Lowe, D. R. Filamentous microfossils from the 3,500-Myr-old Onverwacht Group, Barberton Mountain Land, South Africa. *Nature* **314,** 530–532 (1985).
14. Byerly, G. R., Lowe, D. R. & Walsh, M. M. Stromatolites from the 3,300–3,500-Myr Swaziland Supergroup, Barberton Mountain Land, South Africa. *Nature* **319,** 489–491 (1986).
15. Furnes, H., Banerjee, N. R., Muehlenbachs, K., Staudigel, H. & de Wit, M. Early life recorded in Archean pillow lavas. *Science* **304,** 578–581 (2004).
16. Lowe, D. R. & Byerly, G. R. in *Earth's Oldest Rocks* (eds van Kranendonk, M. J., Smithies, R. H. & Bennet, V. C.) 481–526 (Elsevier, Developments in Precambrian Geology 15, 2007).
17. Tice, M. M., Bostick, B. C. & Lowe, D. R. Thermal history of the 3.5–3.2 Ga Onverwacht and Fig Tree Groups, Barberton greenstone belt, South Africa, inferred by Raman microspectroscopy of carbonaceous material. *Geology* **32,** 37–40 (2004).
18. Lowe, D. R. in *Geologic Evolution of the Barberton Greenstone Belt, South Africa* (eds Lowe, D. R. & Byerly, G. R.) *Geol. Soc. Am. Spec. Pap.* **329,** 83–114 (1999).
19. Hofmann, A. & Bolhar, R. Carbonaceous cherts in the Barberton Greenstone Belt and their significance for the study of early life in the Archean record. *Astrobiology* **7,** 355–388 (2007).
20. Hofmann, A. & Harris, C. Silica alteration zones in the Barberton greenstone belt: a window into subseafloor processes 3.5–3.3 Ga ago. *Chem. Geol.* **257,** 221–239 (2008).
21. van den Boorn, S. H. J. M., van Bergen, M. J., Nijman, W. & Vroon, P. Z. Dual role of seawater and hydrothermal fluids in Early Archean chert formation: evidence from silicon isotopes. *Geology* **35,** 939–942 (2007).
22. Vennemann, T. W., Fricke, H. C., Blake, R. E., O'Neil, J. R. & Colman, A. Oxygen isotope analysis of phosphates: a comparison of techniques for analysis of Ag_3PO_4. *Chem. Geol.* **185,** 321–336 (2002).
23. Berner, R. A. Phosphate removal from sea water by adsorption on volcanogenic ferric oxides. *Earth Planet. Sci. Lett.* **18,** 77–86 (1973).
24. Smith, H. S., O'Neil, J. R. & Erlank, A. J. in *Archean Geochemistry* (eds Kroner, A., Hanson, G. N. & Goodwin, A. M.) 115–137 (Springer, 1984).
25. Jaffrés, J. B. D., Shields, G. A. & Wallmann, K. The oxygen isotope evolution of seawater: a critical review of a long-standing controversy and an improved geological water cycle model for the past 3.4 billion years. *Earth Sci. Rev.* **83,** 83–122 (2007).
26. Longinelli, A. & Nuti, S. Revised phosphate-water isotopic temperature scale. *Earth Planet. Sci. Lett.* **19,** 373–376 (1973).
27. Kolodny, Y., Luz, B. & Navon, O. Oxygen isotope variations in phosphate of biogenic apatites. I. Fish bone apatite—rechecking the rules of the game. *Earth Planet. Sci. Lett.* **64,** 398–404 (1983).
28. Widdel, F. *et al.* Ferrous iron oxidation by anoxygenic phototrophic bacteria. *Nature* **362,** 834–836 (1993).
29. Kappler, A., Pasquero, C., Konhauser, K. O. & Newman, D. K. Deposition of banded iron formations by anoxygenic phototrophic Fe(II)-oxidizing bacteria. *Geology* **33,** 865–868 (2005).
30. Bjerrum, C. J. & Canfield, D. E. Ocean productivity before about 1.9 Gyr ago limited by phosphorus adsorption onto iron oxides. *Nature* **417,** 159–162 (2002).

Supplementary Information is linked to the online version of the paper at www.nature.com/nature.

Acknowledgements We thank M. Kastner and J. R. O'Neil for editorial suggestions and G. Olack and K. Fornash for technical assistance with isotopic analyses.

Author Contributions R.B. and A.L. conceived the study; A.L. performed field work, sample collection, petrographic and chemical analyses; S.J.C. and R.B. developed methods of sequential PO_4 extraction, purification, micro-precipitation and PO_4 oxygen isotope analysis. All authors contributed to the interpretation of results and the writing and editing of the manuscript.

Author Information Reprints and permissions information is available at www.nature.com/reprints. The authors declare no competing financial interests. Correspondence and requests for materials should be addressed to R.B. (ruth.blake@yale.edu).

METHODS

Extraction and purification of PO_4. Phosphate was extracted sequentially from 2–31 g of powdered rock using 10 M HNO_3 (4–7 ml per gram of sample), followed by 6 M HCl (4–11 ml per gram of sample) with continuous agitation on a reciprocal shaker for three and seven days, respectively. The use of HNO_3 and HCl as opposed to hydrofluoric acid and citrate-dithionite-bicarbonate solution[31,32] avoided excessive dissolution of silica and introduction of iron species, respectively, which interfere with subsequent steps in the purification and precipitation of silver phosphate (Ag_3PO_4). Following each extraction, acidic supernatants were separated from residual solids by centrifugation at ~1,950*g* for 20 min, then residual solids were rinsed with deionized water (4–10 ml per gram of sample). The concentrations of PO_4 in acid extractant and rinse solutions were determined colorimetrically[33], and then solutions were pooled for subsequent purification steps.

A single purification method cannot normally achieve separation of extracted phosphate from all contaminants (such as Si, Fe, organic matter). Thus, a combination of several purification steps was used as follows: (1) two rounds of magnesium-induced co-precipitation (MAGIC) of PO_4, (2) micro-precipitation of ammonium phosphomolybdate (APM), (3) recrystallization of APM as magnesium ammonium phosphate (MAP), (4) cation resin, (5) anion resin, (6) second cation resin and (7) final micro-precipitation of Ag_3PO_4.

The MAGIC treatment was adapted from ref. 34 to concentrate extracted phosphate in a <30 ml volume and simultaneously remove interfering ions (for example, Cl^-). Acid solutions containing 5–10 μmol PO_4 were diluted to ~700 ml, which also increased the pH. Solutions were then amended with $Mg(NO_3)_2{\cdot}6H_2O$ to achieve an approximate seawater concentration of 55 mM and 5 M NaOH was added to raise the pH to ~10 to induce Mg- and Fe-hydroxide precipitation. Next, samples were centrifuged for 20 min at 2,600*g* and 25 °C, followed by measurement of the PO_4 concentration of the supernatant to ensure complete co-precipitation/adsorption of PO_4. The residual PO_4/Mg- and Fe-hydroxide pellet was dissolved in a minimum of 10 M HNO_3 (<30 ml) with shaking (reciprocal shaker) at room temperature (21 ± 1 °C) until the pellet dissolved completely. ^{18}O-labelled water, which was added to 10 M HNO_3 solutions, was not incorporated into dissolved phosphate (that is, no phosphate–water exchange occurred) at room temperature (21 ± 1 °C) over a 115-day period (Supplementary Table 3). Thus, the approximately 1-week dissolution period did not introduce artefacts. The dissolved pellet solution was then diluted to ~100 ml in preparation for the second round of MAGIC.

APM and MAP micro-precipitations were adapted from refs 27 and 35. To precipitate 5–10 μmol phosphate as APM, it is critical to constrain the volume of sample solutions below ~5 ml. Thus, the dissolved pellet solution volume was reduced by evaporation below 60 °C for up to 10 h. Oxygen isotope exchange between dissolved PO_4 and water in 10 M HNO_3 at 70 °C is negligible for up to 22 h (Supplementary Table 3). Next, ammonium nitrate (NH_4NO_3) was added to give a NH_4NO_3/PO_4 ratio of 120:1 (by weight). Sample tubes were then heated to 48 °C, followed by slow addition of ~1 ml of ammonium molybdate reagent (100 g MoO_3, 400 ml of 69% HNO_3, 80 ml of 28.0–30.0% NH_4OH and 1 litre distilled water) with constant mixing until yellow APM crystals were formed. After ~30 min, additional reagent (total 7 ml) was added rapidly. APM crystals were allowed to develop overnight at room temperature, then collected and rinsed with 5% (w/w) NH_4NO_3 using a vacuum filtration system and 0.2 μm Gelman Supor filters. APM crystals were dissolved with ~1 ml of ammonium citrate reagent (5 g citric acid, 70 ml of 28.0–30.0% NH_4OH, and 150 ml distilled water) plus deionized water. For MAP precipitation, the initial sample volume was constrained to <2 ml. Magnesia reagent (63.08 g l^{-1} $Mg(NO_3)_2{\cdot}6H_2O$, 149.63 g l^{-1} NH_4NO_3 and 1:50 (by volume) of 28.0–30.0% NH_4OH) was added after adjusting the sample pH to <7 with 10 M HNO_3 to give a ratio of 0.25 ml magnesia reagent per milligram PO_4. Samples were constantly swirled while slowly adding 1:1 (by volume) NH_4OH, until white MAP crystals were formed. After ~30 min, 1 ml of 1:1 (by volume) NH_4OH was added to rapidly precipitate the remaining MAP, which was left to digest overnight at room temperature. MAP crystals were filtered and rinsed with 1:20 (by volume) NH_4OH and then dissolved with ~0.5 ml of 1 M HNO_3 plus deionized water. Next, samples were adjusted to ~pH 5 by addition of 1 M NaOH then loaded onto cation resin columns (Bio-Rad AG50W-X8, H^+ form, 100–200 mesh). Following sample elution, the cation resin was rinsed carefully with deionized water to remove all dissolved PO_4. Next, anion resin treatment followed the methods of ref. 36 as adapted from ref. 37. Samples were adjusted to pH 4–6 by addition of 1 M NaOH, then loaded onto anion resin columns (Bio-Rad AG1-X8, OH^- form, 200–400 mesh; converted to HCO_3^- form with 1 M $NaHCO_3$). Phosphate was eluted from columns using ~30 ml of 0.2 M $NaHCO_3$ at a flow rate of 1 ml min^{-1}. This allowed separation of the phosphate peak from interfering anion peaks. The eluted phosphate peak fractions were treated again with cation resin (H^+ form, ~1 ml resin per 5 ml sample) in batch mode for several hours to remove excess carbonate (evolved as CO_2 gas). The sample solution was next filtered through glass wool and the resin was rinsed with deionized water. Next, sample volume was reduced to ~0.5 ml by evaporation below 60 °C in preparation for the micro-precipitation of silver phosphate.

Micro-precipitation of silver phosphate. Sample solution and rinse water (~1 ml) were transferred to a micro-precipitation vessel. 0.75 ml of Ag-ammine reagent (0.067 M $AgNO_3$, 0.12 M NH_4NO_3 and 0.43 M NH_4OH) was added for every 5 μmol of dissolved PO_4. For samples containing more than 5 μmol PO_4, additional Ag-ammine reagent was added to maintain a Ag:P ratio close to 10. The vessels were incubated overnight at 50 °C to promote formation of large Ag_3PO_4 crystals, which are easier to manipulate in subsequent steps. Ag_3PO_4 crystals were rinsed with deionized water followed by ethanol and dried at 60 °C overnight. Yields of phosphate were above 96%. We tested selected samples (AL03-13D2 and AL03-28I) for the presence of condensed or organophosphates using ^{18}O-labelled waters ($\delta^{18}O_W = -6‰$ and +114.4‰) to prepare extractant solutions. The $\delta^{18}O_P$ values of these samples were identical within error (Supplementary Table 1). This result indicates that incorporation of oxygen from water into PO_4 during the hydrolysis of any phosphoesters or condensed forms such as polyphosphate that may have been present was negligible. Isotope analyses were carried out at the Earth System Center for Stable Isotope Studies (ESCSIS) at Yale using a Thermo-Chemolysis Elemental Analyser (TC/EA, 1,350 °C) coupled to a Delta +XL continuous-flow isotope ratio monitoring mass spectrometer (Thermo-Finnigan) with precision of ±0.2–0.3‰. Phosphate oxygen-isotope ratios were calibrated against conventional fluorination using three silver phosphate standards according to published methods[22].

31. Ruttenberg, K. C. Development of a sequential extraction method for different forms of phosphorus in marine sediments. *Limnol. Oceanogr.* **37,** 1460–1482 (1992).
32. Poulton, S. W. & Canfield, D. E. Development of a sequential extraction procedure for iron: implications for iron partitioning in continentally derived particulates. *Chem. Geol.* **214,** 209–221 (2005).
33. Murphy, J. & Riley, J. P. A modified single solution method for the determination of phosphate in natural waters. *Anal. Chim. Acta* **27,** 31–36 (1962).
34. Karl, D. M. & Tien, G. MAGIC: A sensitive and precise method for measuring dissolved phosphorus in aquatic environments. *Limnol. Oceanogr.* **37,** 105–116 (1992).
35. Tudge, A. P. A method of analysis of oxygen isotopes in orthophosphate—its use in the measurement of paleotemperatures. *Geochim. Cosmochim. Acta* **18,** 81–93 (1960).
36. Liang, Y. *Oxygen Isotope Studies of Biogeochemical Cycling of Phosphorus* PhD thesis, Yale Univ. (2005).
37. Colman, S. A. *The Oxygen Isotope Composition of Dissolved Inorganic Phosphate and the Marine Phosphorus Cycle* PhD thesis, Yale Univ. (2002).